Nuclear effects in protonium formation low-energy three-body reaction: $\bar{p} + (p\mu)_{1s} \rightarrow (\bar{p}p)_{\alpha} + \mu^{-}$

Strong $\bar{p}-p$ interaction in $\bar{p} + (p\mu)_{1s}$

Renat A. Sultanov[1,a] and Dennis Guster[b]

[1] *Department of Information Systems, BCRL & Integrated Science and Engineering Laboratory Facility (ISELF) at St. Cloud State University, St. Cloud, MN 56301-4498, USA*

Abstract. A three-charge-particle system ($\bar{p}$, μ^{-}, p^{+}) with an additional matter-antimatter, i.e. $\bar{p}-p^{+}$, nuclear interaction is the subject of this work. Specifically, we carry out a few-body computation of the following protonium formation reaction: $\bar{p} + (p^{+}\mu^{-})_{1s} \rightarrow (\bar{p}p^{+})_{1s} + \mu^{-}$, where p^{+} is a proton, $\bar{p}$ is an antiproton, μ^{-} is a muon, and a bound state of p^{+} and its counterpart $\bar{p}$ is a protonium atom: $Pn = (\bar{p}p^{+})$. The low-energy cross sections and rates of the Pn formation reaction are computed in the framework of a Faddeev-like equation formalism. The strong $\bar{p}-p^{+}$ interaction is approximately included in this calculation.

1 Introduction

Obtaining and storing of low-energy antiprotons ($\bar{p}$) is of significant scientific and practical interest and importance in current research in atomic and nuclear physics [1–4]. For example, with the use of slow $\bar{p}$'s it would be possible to make low temperature ground state antihydrogen atoms $\bar{H}_{1s}$ - a bound state of $\bar{p}$ and e^{+}, i.e. a positron. The two-particle atom represents the simplest and stable anti-matter species. By comparing the properties of the hydrogen atom H and $\bar{H}$ it would be possible to test the fundamentals of physics, such as CPT theorem [5]. In this connection it is important to mention the metastable antiprotonic helium atoms too, i.e. atomcules, such as $\bar{p}^{3}He^{+}$ and $\bar{p}^{4}He^{+}$ [6]. In the field of the $\bar{p}$ physics these Coulomb three-body systems play a very important role. For example, with the use of high-precision laser spectroscopy atomclues allow us to measure $\bar{p}$'s charge-to-mass ratio and other fundamental constants in the standard model [7].

Together with the atomcules and the $\bar{H}$ atoms there is now a significant interest in protonium (Pn) atom too: a bound state of $\bar{p}$ and p^{+} [8–10]. The two-particle system is also named as antiprotonic hydrogen. In the atomic scale it is a heavy and a very small system with strong Coulomb and nuclear interactions. An interplay between these interactions occurs inside the atom. The last circumstance is responsible for interesting resonance and quasi-bound states in Pn [11]. Therefore, Pn represents a very useful tool to study, for example, the anti-nucleon−nucleon ($\bar{N}N$) interaction potential [12, 13] and annihilation processes [14, 15]. Additionally, as we already mentioned, the interplay between Coulomb and nuclear forces plays a significant role in the $\bar{p}$ and p quantum dynamics [16]. The $\bar{p}+p^{+}$

[a] e-mail: rasultanov@stcloudstate.edu
[b] e-mail: dcguster@stcloudstate.edu

elastic scattering has also been considered in many papers, see for example review [14]. Additionally, *Pn* formation is related to charmonium - a hydrogen-like atom ($\bar{c}c$), i.e. a bound state of a c-antiquark ($\bar{c}$) and c-quark [17]. Because of the fundamental importance of protonium and problems related to its formation, as far as bound and quasi-bound states, resonances and spectroscopy, the two-particle atom have attracted much attention last decades.

There are a number of few-body collisions to make *Pn* atoms at low temperatures. For example, the following three-charge-particle reaction is one of them:

$$\bar{\mathrm{p}} + (\mathrm{p}^+ e^-)_{1s} \rightarrow (\bar{\mathrm{p}}\mathrm{p}^+)_{\alpha'} + e^-, \tag{1}$$

First of all, this collision represents a Coulomb three-body system and has been considered in many theoretical works in which different methods and computational techniques have been applied [18–20]. We also would like to point out, that because in the process (1) a heavy particle, i.e. proton, is transferred from one negative "center", e^-, to another, $\bar{\mathrm{p}}$, it would be difficult to apply a computational method based on an adiabatic (Born-Oppenheimer) approach [21]. Additionally, it would be useful to mention here, that experimentalists use another few-body reaction to produce *Pn* atoms, i.e. a collision between a slow $\bar{\mathrm{p}}$ and a positively charged molecular hydrogen ion, i.e. H_2^+:

$$\bar{\mathrm{p}} + \mathrm{H}_2^+ \rightarrow (\bar{\mathrm{p}}\mathrm{p}^+)_{\alpha'} + \mathrm{H}. \tag{2}$$

In the current work, however, we consider another three-body system of the *Pn* formation reaction. Specifically, we compute the cross-sections and rates of a very low energy collision between $\bar{\mathrm{p}}$ and a muonic hydrogen atom H_μ, i.e. a bound state of p^+ and a negative muon:

$$\bar{\mathrm{p}} + (\mathrm{p}\mu)_{1s} \rightarrow (\bar{\mathrm{p}}\mathrm{p}^+)_{\alpha} + \mu^-. \tag{3}$$

Here, α=1s, 2s or 2p is *Pn*'s final quantum atomic state. Because of the μ^- participation in the reaction (3), at very low energy collisions *Pn* can be formed in an extremely small size (compact in the atomic scale) ground and close to ground states α. In these states the hadronic nuclear forces between $\bar{\mathrm{p}}$ and p are much stronger than in the reaction (1) and, probably, would be very effective in order to study them. The size of the *Pn* atom in its ground state is only $a_0(Pn) = \hbar^2/(e_0^2 m_p/2) \sim 50$ fm! At such small distances the Coulomb interaction between $\bar{\mathrm{p}}$ and p^+ becomes extremely strong. The corresponding binding energy in the *Pn* atom without the inclusion of the nuclear $\bar{\mathrm{p}}$–p^+ interaction is $E_n(Pn) = -e_0^4 m_p/2/(2\hbar n^2) \sim -10$ keV. Here, we took $n = 1$, $\hbar$ is the Planck constant, e_0 is the electron charge, and m_p is the proton mass. In connection with this we would like to make a comment. The real $\bar{\mathrm{p}}$–p^+ binding energy, i.e. with inclusion of the strong interaction, can have a large value. This value may be comparable or even larger than m_p. Therefore, it might be necessary to use a relativistic treatment to the reaction (3) in the output channel [22]. The situation with very strong Coulomb interaction inside *Pn* can also be a reason of vacuum polarization forces. The Casimir forces can contribute (it might be quite significant) to the final cross sections and rates of the *Pn* formation reaction (3). It would be interesting to take into account all these physical effects in the framework of the reaction (3) and compute their influence on its rate. Hopefully, soon experimentalists will be able to carry out high quality measurements of the reaction (3). Thereafter one could compare the new results with corresponding theoretical data and fit (adjust) the $\bar{\mathrm{p}}$–p^+ strong interaction in the framework of the theoretical calculations in order to reproduce the laboratory data. This would allow us to better know and understand the strong $\bar{\mathrm{p}}$–p^+ interaction and the annihilation processes.

In the first order approximation reaction (3) can be considered as a three-charged-particle system (123) with arbitrary and comparable masses: m_1, m_2, and m_3. It is shown in Fig. 1. The strong $\bar{\mathrm{p}}$–p^+ interaction can be included approximately after a solution of the Coulomb three-body problem. A few-body method based on a Faddeev-like equation formalism is applied. In this approach

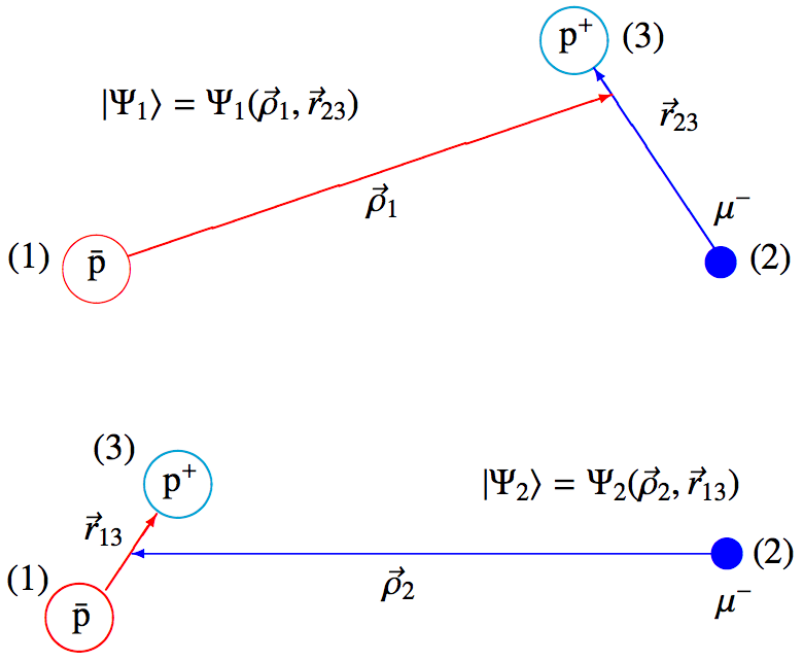

Figure 1. Two asymptotic spacial configurations of the 3-body system (123), or more specifically $(\bar{p}, \mu^-, p^+)$ which is considered in this work. The few-body Jacobi coordinates $(\vec{\rho}_i, \vec{r}_{jk})$, where $i \neq j \neq k = 1, 2, 3$ are also shown together with the 3-body wave function components Ψ_1 and Ψ_2: $\Psi = \Psi_1 + \Psi_2$ is the total wave function of the 3-body system.

the three-body wave function is decomposed in two independent Faddeev-type components [23, 24]. Each component is determined by its own independent Jacobi coordinates. Since, the reaction (3) is considered at low energies, i.e. well below the three-body break-up threshold, the Faddeev-type components are quadratically integrable over the internal target variables $\vec{r}_{23}$ and $\vec{r}_{13}$. They are shown in Fig. 1.

The next section represents the notation pertinent to the three-charged-particle system (123), the basic few-body equations, boundary conditions, detailed derivation of the set of coupled one-dimensional integral-differential equations suitable for numerical calculations and the numerical computational approach used in the current paper. The muonic units, i.e. $e = \hbar = m_\mu = 1$, are used in this work, where $m_\mu = 206.769\ m_e$ is the mass of the muon. The proton (anti-proton) mass is $m_p = m_{\bar{p}}$=1836.152 m_e.

2 A three-charge-particle system: $\bar{p}$, μ^- and p^+

As we already mentioned in Introduction, a quantum-mechanical few-body approach is applied in this work. A coordinate space representation is used. This approach is based on a reduction of the total three-body wave function Ψ on two or three Faddeev-type components [24]. When one has two negative and one positive charges, only two asymptotic configurations are possible below the total energy break-up threshold. The situation is explained in Fig. 1 in the case of the title three-body system.

Therefore, one can decompose Ψ only on two components and write down a set of two coupled equations [25, 26]. A modified close coupling method is applied in order to solve these equations [27–29]. This means to carry out an expansion of the Faddeev-type components into eigenfunctions of the subsystem Hamiltonians. This technique provides an infinite set of one-dimensional integral-differential equations [30, 31]. Within this formalism the asymptotic of the full three-body wave function contains two parts corresponding to two open channels [32].

2.1 An infinite set of coupled integral-differential few-body equations

One could use the following system of units: $e = \hbar = m_3 = 1$. We denote antiproton $\overline{\mathrm{p}}$ by 1, a negative muon μ^- by 2, and a proton p^+ by 3. Before the three-body breakup threshold two cluster asymptotic configurations are possible in the three-body system, i.e. (23)−1 and (13)−2. As we mentioned above, by their own Jacobi coordinates $\{\vec{r}_{j3}, \vec{\rho}_k\}$ as shown in Fig. 1:

$$\vec{r}_{j3} = \vec{r}_3 - \vec{r}_j, \quad \vec{\rho}_k = \frac{(\vec{r}_3 + m_j \vec{r}_j)}{(1 + m_j)} - \vec{r}_k, \quad (j \neq k = 1, 2). \tag{4}$$

Here $\vec{r}_\xi$, m_ξ are the coordinates and the masses of the particles $\xi = 1, 2, 3$ respectively. This suggests a Faddeev formulation which uses only two components. A general procedure to derive such formulations is described in work [25]. In this approach the three-body wave function is represented as follows:

$$|\Psi\rangle = \Psi_1(\vec{r}_{23}, \vec{\rho}_1) + \Psi_2(\vec{r}_{13}, \vec{\rho}_2), \tag{5}$$

where each Faddeev-type component is determined by its own Jacobi coordinates. Moreover, $\Psi_1(\vec{r}_{23}, \vec{\rho}_1)$ is quadratically integrable over the variable $\vec{r}_{23}$, and $\Psi_2(\vec{r}_{13}, \vec{\rho}_2)$ over the variable $\vec{r}_{13}$. To define $|\Psi_l\rangle$, $(l = 1, 2)$ a set of two coupled Faddeev-Hahn-type equations can be written:

$$\Big(E - \hat{H}_0 - V_{23}(\vec{r}_{23})\Big)\Psi_1(\vec{r}_{23}, \vec{\rho}_1) = \Big(V_{23}(\vec{r}_{23}) + V_{12}(\vec{r}_{12})\Big)\Psi_2(\vec{r}_{13}, \vec{\rho}_2), \tag{6}$$

$$\Big(E - \hat{H}_0 - V_{13}(\vec{r}_{13})\Big)\Psi_2(\vec{r}_{13}, \vec{\rho}_2) = \Big(V_{13}(\vec{r}_{13}) + V_{12}(\vec{r}_{12})\Big)\Psi_1(\vec{r}_{23}, \vec{\rho}_1). \tag{7}$$

Here, $\hat{H}_0$ is the kinetic energy operator of the three-particle system, $V_{ij}(r_{ij})$ are paired interaction potentials $(i \neq j = 1, 2, 3)$, E is the total energy.

Now, let us present the equations (6)-(7) in terms of the adopted notation

$$\Big(E + \frac{1}{2M_k}\triangle_{\vec{\rho}_k} + \frac{1}{2\mu_j}\triangle_{\vec{r}_{j3}} - V_{j3}\Big)\Psi_i(\vec{r}_{j3}, \vec{\rho}_k) = \Big(V_{j3} + V_{jk}\Big)\Psi_{i'}(\vec{r}_{k3}, \vec{\rho}_j\Big), \tag{8}$$

here $i \neq i' = 1, 2$, $M_k^{-1} = m_k^{-1} + (1 + m_j)^{-1}$ and $\mu_j^{-1} = 1 + m_j^{-1}$. In order to separate angular variables, the wave function components Ψ_i are expanded over bipolar harmonics:

$$\{Y_\lambda(\hat{\rho}) \otimes Y_l(\hat{r})\}_{LM} = \sum_{\mu m} C^{LM}_{\lambda\mu lm} Y_{\lambda\mu}(\hat{\rho}) Y_{lm}(\hat{r}), \tag{9}$$

where $\hat{\rho}$ and $\hat{r}$ are angular coordinates of vectors $\vec{\rho}$ and $\vec{r}$; $C^{LM}_{\lambda\mu lm}$ are Clebsh-Gordon coefficients; Y_{lm} are spherical functions [33]. The configuration triangle of the particles (123) is presented in Fig. 2 together with the Jacobi coordinates $\{\vec{r}_{23}, \vec{\rho}_1\}$ and $\{\vec{r}_{13}, \vec{\rho}_2\}$ and angles between them. The centre-of-mass of the whole three-body system is designated as O. The centre-of-masses of the two-body subsystems (23) and (13) are O_1 and O_2 respectively. Substituting the following expansion:

$$\Psi_i(\vec{r}_{j3}, \vec{\rho}_k) = \sum_{LM\lambda l} \Phi^i_{LM\lambda l}(\rho_k, r_{j3}) \Big\{Y_\lambda(\hat{\rho}_k) \otimes Y_l(\hat{r}_{j3})\Big\}_{LM} \tag{10}$$

into (8), multiplying this by the appropriate biharmonic functions and integrating over the corresponding angular coordinates of the vectors $\vec{r}_{j3}$ and $\vec{\rho}_k$, we obtain a set of equations which for the case of the central potentials has the form:

$$\Big(E + \frac{1}{2M_k\rho_k^2}\Big\{\frac{\partial}{\partial\rho_k}(\rho_k^2\frac{\partial}{\partial\rho_k}) - \lambda(\lambda+1)\Big\} + \frac{1}{2\mu_j r_{j3}^2}\Big\{\frac{\partial}{\partial r_{j3}}(r_{j3}^2\frac{\partial}{\partial r_{j3}}) - l(l+1)\Big\}$$
$$-V_{j3}\Big)\Phi^i_{LM\lambda l}(\rho_k, r_{j3}) = \int d\hat{\rho}_k \int d\hat{r}_{j3} \sum_{\lambda' l'} W^{(ii')LM}_{\lambda l\lambda' l'}\Phi^{i'}_{LM\lambda' l'}(\rho_j, r_{k3}), \tag{11}$$

where the following notation has been introduced:

$$W^{(ii')LM}_{\lambda l\lambda' l'} = \Big\{Y_\lambda(\hat{\rho}_k)\otimes Y_l(\hat{r}_{j3})\Big\}^*_{LM}\Big(V_{j3}+V_{jk}\Big)\Big\{Y_{\lambda'}(\hat{\rho}_j)\otimes Y_{l'}(\hat{r}_{k3})\Big\}_{LM}. \tag{12}$$

To progress from (11) to one-dimensional equations, we apply a modified close coupling method, which consists of expanding each component of the wave function $\Psi_i(\vec{r}_{j3}, \vec{\rho}_k)$ over the Hamiltonian eigenfunctions of subsystems:

$$\hat{h}_{j3} = -\frac{1}{2\mu_j}\nabla^2_{\vec{r}_{j3}} + V_{j3}(\vec{r}_{j3}). \tag{13}$$

Thus, following expansions can be applied:

$$\Phi^i_{LM\lambda l}(\rho_k, r_{j3}) = \frac{1}{\rho_k}\sum_n f^{(i)LM}_{nl\lambda}(\rho_k)R^{(i)}_{nl}(r_{j3}), \tag{14}$$

where functions $R^i_{nl}(r_{j3})$ are defined by the following equation:

$$\Big(E^i_n + \frac{1}{2\mu_j r_{j3}^2}\Big\{\frac{\partial}{\partial r_{j3}}(r_{j3}^2\frac{\partial}{\partial r_{j3}}) - l(l+1)\Big\} - V_{j3}\Big)R^i_{nl}(r_{j3}) = 0. \tag{15}$$

Substituting Eq. (14) into (11), multiplying by the corresponding functions $R^i_{nl}(r_{j3})$ and integrating over $r^2_{j3}dr_{j3}$ yields a set of integral-differential equations for the unknown functions $f^i_{nl\lambda}(\rho_k)$:

$$2M_k(E-E^i_n)f^i_\alpha(\rho_k) + \Big(\frac{\partial^2}{\partial\rho_k^2} - \frac{\lambda(\lambda+1)}{\rho_k^2}\Big)f^i_\alpha(\rho_k) = 2M_k\sum_\alpha\int_0^\infty dr_{j3}r^2_{j3}\int d\hat{r}_{j3}\int d\hat{\rho}_k\rho_k\rho_j \times \frac{Q^{ii'}_{\alpha\alpha'}f^{i'}_{\alpha'}(\rho_j)}{\rho_j}, \tag{16}$$

where

$$Q^{ii'}_{\alpha\alpha'} = R^i_{nl}(r_{j3})W^{(ii')LM}_{\lambda l\lambda' l'}R^{i'}_{n'l'}(r_{k3}). \tag{17}$$

For brevity one can denote $\alpha \equiv nl\lambda$ ($\alpha' \equiv n'l'\lambda'$), and omit LM because all functions have to be the same. The functions $f^i_\alpha(\rho_k)$ depend on the scalar argument, but this set is still not one-dimensional, as formulas in different frames of the Jacobi coordinates:

$$\vec{\rho}_j = \vec{r}_{j3} - \beta_k\vec{r}_{k3}, \quad \vec{r}_{j3} = \frac{1}{\gamma}(\beta_k\vec{\rho}_k + \vec{\rho}_j), \quad \vec{r}_{jk} = \frac{1}{\gamma}(\sigma_j\vec{\rho}_j - \sigma_k\vec{\rho}_k), \tag{18}$$

with the following mass coefficients:

$$\beta_k = m_k/(1+m_k), \quad \sigma_k = 1-\beta_k, \quad \gamma = 1-\beta_k\beta_j \ \ (j\neq k = 1,2), \tag{19}$$

clearly demonstrate that the modulus of $\vec{\rho}_j$ depends on two vectors, over which integration on the right-hand sides is accomplished: $\vec{\rho}_j = \gamma\vec{r}_{j3} - \beta_k\vec{\rho}_k$. Therefore, to obtain one-dimensional integral-differential equations, corresponding to equations (16), we will proceed with the integration over variables $\{\vec{\rho}_j, \hat{\rho}_k\}$, rather than $\{\vec{r}_{j3}, \hat{\rho}_k\}$. The Jacobian of this transformation is γ^{-3}. Thus, we arrive at a set of one-dimensional integral-differential equations:

$$2M_k(E - E_n^i)f_\alpha^i(\rho_k) + \Big(\frac{\partial^2}{\partial\rho_k^2} - \frac{\lambda(\lambda+1)}{\rho_k^2}\Big)f_\alpha^i(\rho_k) = \frac{M_k}{\gamma^{-3}}\sum_{\alpha'}\int_0^\infty d\rho_j S_{\alpha\alpha'}^{ii'}(\rho_j,\rho_k)f_{\alpha'}^{i'}(\rho_j), \tag{20}$$

where functions $S_{\alpha\alpha'}^{ii'}(\rho_j,\rho_k)$ are defined as follows:

$$S_{\alpha\alpha'}^{ii'}(\rho_j,\rho_k) = 2\rho_j\rho_k\int d\hat{\rho}_j\int d\hat{\rho}_k R_{nl}^i(r_{j3})\left\{Y_\lambda(\hat{\rho}_k)\otimes Y_l(\hat{r}_{j3})\right\}_{LM}^*\Big(V_{j3}+V_{jk}\Big) \times\left\{Y_{\lambda'}(\hat{\rho}_j)\otimes Y_{l'}(\hat{r}_{k3})\right\}_{LM} R_{n'l'}^{i'}(r_{k3})\ . \tag{21}$$

In the next section we show that fourfold multiple integration in equations (21) leads to a one-dimensional integral and the expression (21) could be determined for any orbital momentum value L:

$$S_{\alpha\alpha'}^{ii'}(\rho_j,\rho_k) = \frac{4\pi}{2L+1}[(2\lambda+1)(2\lambda'+1)]^{\frac{1}{2}}\rho_j\rho_k\int_0^\pi d\omega\sin\omega R_{nl}^i(r_{j3})\Big(V_{j3}(r_{j3}) +V_{jk}(r_{jk})\Big)R_{n'l'}^{i'}(r_{k3})\sum_{mm'}D_{mm'}^L(0,\omega,0)C_{\lambda 0lm}^{Lm}C_{\lambda' 0l'm'}^{Lm'}Y_{lm}(\nu_j,\pi)Y_{l'm'}^*(\nu_k,\pi)\ , \tag{22}$$

where $D_{mm'}^L(0,\omega,0)$ are Wigner functions, ω is the angle between $\vec{\rho}_j$ and $\vec{\rho}_k$, ν_j is the angle between $\vec{r}_{k3}$ and $\vec{\rho}_j$, ν_k is the angle between $\vec{r}_{j3}$ and $\vec{\rho}_k$ (please see Fig. 2). Finally, we obtain an infinite set of coupled integral-differential equations for the unknown functions $f_\alpha^1(\rho_1)$ and $f_{\alpha'}^2(\rho_2)$ [31], i.e. $f_{\alpha(\alpha')}^{i(i')}(\rho_{i(i')})$ ($i \neq i' = 1,2$), α and α' belong to two different sets of three-body quantum numbers:

$$\Big((k_n^i)^2 + \frac{\partial^2}{\partial\rho_i^2} - \frac{\lambda(\lambda+1)}{\rho_i^2}\Big)f_\alpha^i(\rho_i) = g\sum_{\alpha'}\sqrt{\frac{(2\lambda+1)(2\lambda'+1)}{(2L+1)}}\int_0^\infty d\rho_{i'}f_{\alpha'}^{i'}(\rho_{i'})\int_0^\pi d\omega\sin\omega \times R_{nl}^i(r_{i'3})\Big(V_{i'3}(r_{i'3}) + V_{ii'}(r_{ii'})\Big)R_{n'l'}^{i'}(r_{i3})\rho_{i'}\rho_i\sum_{mm'}D_{mm'}^L(0,\omega,0)C_{\lambda 0lm}^{Lm}C_{\lambda' 0l'm'}^{Lm'}Y_{lm}(\nu_i,\pi)Y_{l'm'}^*(\nu_{i'},\pi). \tag{23}$$

The total angular momentum of the three-body system is L. Next in Eq. (23):

$$g = \frac{4\pi M_i}{\gamma^3}, \quad k_n^i = \sqrt{2M_i(E - E_n^{i'})}, \tag{24}$$

where $E_n^{i'}$ is the binding energy of the subsystem $(i'3)$. Also:

$$M_1 = \frac{m_1(m_2+m_3)}{(m_1+m_2+m_3)} \ \text{ and } \ M_2 = \frac{m_2(m_1+m_3)}{(m_1+m_2+m_3)} \tag{25}$$

are the reduced masses. Further: $D_{mm'}^L(0,\omega,0)$ the Wigner functions, $C_{\lambda 0lm}^{Lm}$ the Clebsh-Gordon coefficients, Y_{lm} are the spherical functions, ω is the angle between the Jacobi coordinates $\vec{\rho}_i$ and $\vec{\rho}_{i'}$, ν_i is

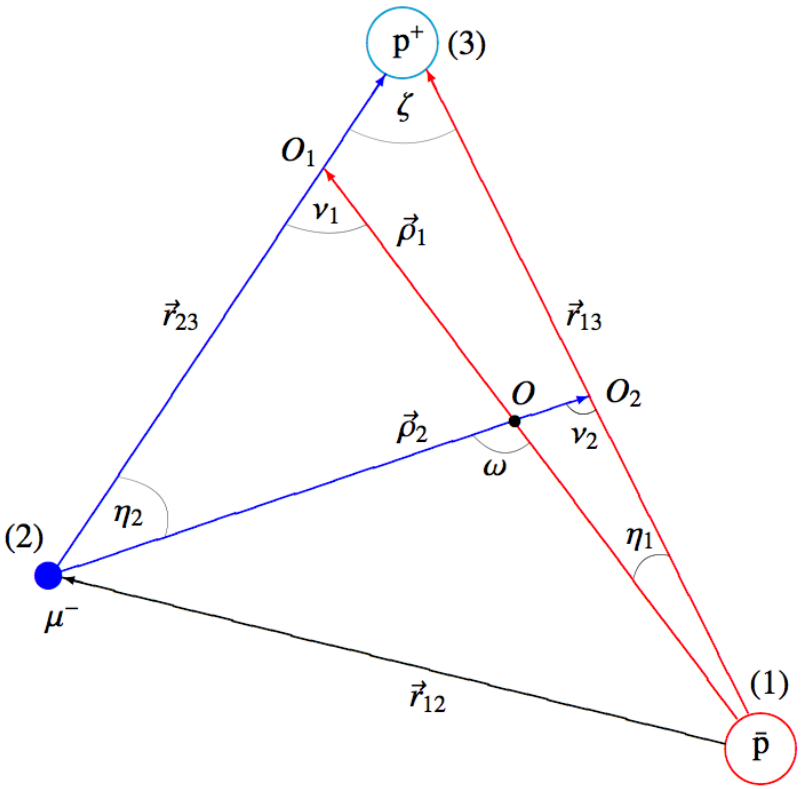

Figure 2. The title three-charge-particle system $\bar{p}, \mu^-$ and p (or p^+ - proton) and system's configurational triangle (123) are shown together with the few-body Jacobi coordinates (vectors): $\{\vec{\rho}_1, \vec{r}_{23}\}$ and $\{\vec{\rho}_2, \vec{r}_{13}\}$. Additionally, $\vec{r}_{12}$ is the vector between two negative particles in the system. The needed for detailed few-body treatment geometrical angles between the vectors such as $\eta_{1(2)}, \nu_{1(2)}, \zeta$ and ω are also presented in this figure.

the angle between $\vec{r}_{i'3}$ and $\vec{\rho}_i$, $\nu_{i'}$ is the angle between $\vec{r}_{i3}$ and $\vec{\rho}_{i'}$. One can show that:

$$\begin{aligned} \sin\nu_i &= \frac{\rho_k}{r_{kj}\gamma}\sin\omega, \\ \cos\nu_i &= \frac{\beta\rho_i + \rho_k\cos\omega}{\gamma r_{kj}}, \\ \gamma &= 1 - \frac{m_i m_{i'}}{(m_i+1)(m_{i'}+1)}. \end{aligned} \tag{26}$$

2.1.1 Angular integrals

The details of the derivation of the angular integrals $S^{ii'}_{\alpha\alpha'}(\rho_j, \rho_k)$ (22) are explained below in this section. The configuration triangle, $\triangle(123)$, is determined by the Jacobi vectors $(\vec{r}_{j3}, \vec{\rho}_k)$ and should be considered in an arbitrary coordinate system $OXYZ$. In this initial system the angle variables of the three-body Jacobi vectors $\{\vec{r}_{j3}, \vec{\rho}_k\}$ have the following values: $\hat{r}_{j3} = (\theta_j, \phi_j)$, $\hat{\rho}_k = (\Theta_k, \Phi_k)$, $j \neq k =$

1, 2. Let us adopt a new coordinate system $O'X'Y'Z'$ in which the axis $O'Z'$ is directed over the vector $\vec{\rho}_k$, $\triangle(123)$ belongs to the plain $O'X'Z'$ and the vertex $k = 1$ of $\triangle(123)$ coincides with the origin O' of the new $OX'Y'Z'$. The new angle variables of the Jacobi vectors in the $O'X'Y'Z'$ system have now the following values: $\hat{r}'_{j3} = (\nu_k, \pi)$, $\hat{\rho}'_k = (0, 0)$, $\hat{r}'_{k3} = (\eta_k, \pi)$, $\hat{\rho}'_j = (\omega, \pi)$, here $k = 1$ and $j = 2$. The spatial rotational transformation from $OXYZ$ to $O'X'Y'Z'$ has been done with the use of the following Euler angles $(\Phi_k, \Theta_k, \varepsilon)$ [33]. Taking into account the transformation rule for the bipolar harmonics between new and old coordinate systems, one can write down the following relationships [33]:

$$\left\{Y_\lambda(\hat{\rho}_k) \otimes Y_l(\hat{r}_{j3})\right\}^*_{LM} = \sum_m (D^L_{Mm}(\Phi_k, \Theta_k, \varepsilon))^* \left\{Y_\lambda(\hat{\rho}'_k) \otimes Y_l(\hat{r}'_{j3})\right\}^*_{Lm} \tag{27}$$

and

$$\left\{Y_{\lambda'}(\hat{\rho}_j) \otimes Y_{l'}(\hat{r}_{k3})\right\}_{LM} = \sum_{m'} D^L_{Mm'}(\Phi_k, \Theta_k, \varepsilon) \left\{Y_{\lambda'}(\hat{\rho}'_j) \otimes Y_{l'}(\hat{r}'_{k3})\right\}_{Lm'}, \tag{28}$$

where $D^L_{Mm}(\Phi_k, \Theta_k, \varepsilon)$ are the Wigner functions [33]. The fourfold multiple angular integration $\int d\hat{\rho}_j \int d\hat{\rho}_k$ in Eq. (21) can be written in the new variables and be symbolically represented as $\int d\hat{\rho}_j \int d\hat{\rho}_k = \int_0^\pi d\omega \sin\omega \int_0^{2\pi} d\varepsilon \int_0^{2\pi} d\Phi_k \int_0^\pi \sin\Theta_k d\Theta_k$. Next, taking into account the normalizing condition for the Wigner functions [33]:

$$\int_0^{2\pi} d\varepsilon \int_0^{2\pi} d\Phi_k \int_0^\pi \sin\Theta_k d\Theta_k (D^L_{Mm}(\Phi_k, \Theta_k, \varepsilon))^* D^L_{Mm'}(\Phi_k, \Theta_k, \varepsilon)) = \frac{8\pi^2}{2L+1}\delta_{mm'} \tag{29}$$

one can obtain the following formula:

$$S^{ii'}_{\alpha\alpha'}(\rho_j, \rho_k) = 2\rho_j\rho_k \sum_m \frac{8\pi^2}{2L+1} \int_0^\pi d\omega \sin\omega R^i_{nl}(r_{j3}) \left\{Y_\lambda(0,0) \otimes Y_l(\hat{r}'_{j3})\right\}^*_{Lm} \times (V_{j3} + V_{jk}) \left\{Y_{\lambda'}(\hat{\rho}'_j) \otimes Y_{l'}(\hat{r}'_{k3})\right\}_{Lm'} R^{i'}_{n'l'}(r_{k3}) . \tag{30}$$

Now, let us make the next transformation of $\triangle(123)$ in which the vertex $j = 2$ of $\triangle(123)$ coincides with the centre O' of the $O'X'Y'Z'$ and $O'XYZ$, however the axis $O'Z''$ is directed along $\vec{\rho}_j$ and $\triangle(123)$ belongs to the plain $O'X''Z''$. This transformation, which converts the coordinate frame $O'X'Y'Z'$ into $O'X''Y''Z''$ is characterized by the following Euler angles $(0, \omega, 0)$. Therefore the vectors $(\vec{r}_{k3}, \vec{\rho}_j)$ have the following new variables: $\hat{r}''_{k3} = (\nu_j, \pi)$, $\hat{\rho}''_j = (0, 0)$. As a result of this rotation one can write down the following relationship:

$$\left\{Y_{\lambda'}(\hat{\rho}'_j) \otimes Y_{l'}(\hat{r}'_{k3})\right\}_{Lm} = \sum_{m'} D^L_{Mm'}(0, \omega, 0) \left\{Y_{\lambda'}(\hat{\rho}''_j) \otimes Y_{l'}(\hat{r}''_{k3})\right\}_{Lm'} \tag{31}$$

and obtain the following result:

$$S^{ii'}_{\alpha\alpha'}(\rho_j, \rho_k) = 2\rho_j\rho_k \sum_{mm'} \frac{8\pi^2}{2L+1} \int d\omega \sin\omega R^i_{nl}(r_{j3}) \left\{Y_\lambda(0,0) \otimes Y_l(\hat{r}'_{j3})\right\}^*_{Lm} (V_{j3} + V_{jk}) \times D^L_{mm'}(0, \omega, 0) \left\{Y_{\lambda'}(0,0) \otimes Y_{l'}(\hat{r}''_{k3})\right\}_{Lm'} R^{i'}_{n'l'}(r_{k3}). \tag{32}$$

Now by taking into account that $Y_{lm}(0, 0) = \delta_{m,0}\sqrt{(2l+1)/4\pi}$ [33], the bipolar harmonics in (32) are:

$$\{Y_\lambda(0,0) \otimes Y_l(\nu_k, \pi)\}^*_{Lm} = \sqrt{\frac{2\lambda+1}{4\pi}} C^{Lm}_{\lambda 0 lm} Y^*_{lm}(\nu_k, \pi), \tag{33}$$

$$\left\{Y_{\lambda'}(0,0) \otimes Y_{l'}(\nu_j, \pi)\right\}_{Lm'} = \sqrt{\frac{2\lambda'+1}{4\pi}} C^{Lm'}_{\lambda' 0 l' m'} Y_{l'm'}(\nu_j, \pi), \tag{34}$$

with the use of these relationships we finally get the convenient for numerical computations Eq. (22). In conclusion, we would like to note that rotational transformations of a coordinate system $OXYZ$ might also be useful in the theory of molecular collisions. In addition, few useful formulas for the triangle (123) are presented below: $\sin\nu_1 = \rho_2/(\gamma r_{23})\sin\omega$, $\sin\nu_2 = \rho_1/(\gamma r_{13})\sin\omega$ and $\cos\nu_1 = 1/(\gamma r_{23})(\beta\rho_1 + \rho_2\cos\omega))$, $\cos\nu_2 = 1/(\gamma r_{13})(\alpha\rho_2 + \rho_1\cos\omega))$.

2.2 Boundary conditions, numerics, cross sections and the reaction rates

To find a unique solution to Eqs. (23) appropriate boundary conditions depending on the specific physical situation need to be considered. First we impose:

$$f_{nl}^{(i)}(0) \sim 0. \tag{35}$$

Next, for the three-body charge-transfer problems we apply the well known **K**−matrix formalism. This method has already been applied for solution of three-body problems in the framework of the Schrődinger equation [34, 35] and coordinate space Faddeev equation [36]. For the present rearrangement scattering problem with $i+(j3)$ as the initial state, in the asymptotic region, it takes two solutions to Eq.(23) to satisfy the following boundary conditions:

$$\begin{cases} f_{1s}^{(i)}(\rho_i) \underset{\rho_1\to+\infty}{\sim} \sin(k_1^{(i)}\rho_i) + K_{ii}\cos(k_1^{(i)}\rho_i) \\ f_{1s}^{(j)}(\rho_j) \underset{\rho_j\to+\infty}{\sim} \sqrt{v_i/v_j}K_{ij}\cos(k_1^{(j)}\rho_j)\ , \end{cases} \tag{36}$$

where K_{ij} are the appropriate coefficients, and v_i ($i = 1, 2$) is a velocity in channel i. With the following change of variables in Eq. (23):

$$\mathrm{f}_{1s}^{(i)}(\rho_i) = f_{1s}^{(i)}(\rho_i) - \sin(k_1^{(i)}\rho_i), \tag{37}$$

(i=1, 2) we get two sets of inhomogeneous equations which are solved numerically. The coefficients K_{ij} can be obtained from a numerical solution of the FH-type equations. The cross sections are given by the following expression:

$$\sigma_{ij} = \frac{4\pi}{k_1^{(i)2}}\left|\frac{\mathbf{K}}{1 - i\mathbf{K}}\right|^2 = \frac{4\pi}{k_1^{(i)2}}\frac{\delta_{ij}D^2 + K_{ij}^2}{(D-1)^2 + (K_{11}+K_{22})^2}, \tag{38}$$

where $(i, j = 1, 2)$ refer to the two channels and $D = K_{11}K_{22} - K_{12}K_{21}$. Also, from the quantum-mechanical unitarity principle one can derive that the scattering matrix $\mathbf{K} = \begin{pmatrix} K_{11} & K_{12} \\ K_{21} & K_{22} \end{pmatrix}$ has the following important feature:

$$K_{12} = K_{21}. \tag{39}$$

In this work, the relationship (39) is checked for all considered collision energies in the framework of the 1s, 1s+2s and 1s+2s+2p modified close coupling approximation Eqs. (10) and (14).

The solution of the Eqs. (6)-(7) involving both components $\Psi_{1(2)}$ required that we apply the expansions (10) and (14) over the angle and the distance variables respectively. However, to obtain a numerical solution for the set of coupled Eqs. (23) we only include the -s and -p waves in the expansion (10) and limit n up to 2 in the Eq. (14). As a result we arrive at a truncated set of six coupled integral-differential equations, since in $\Psi_{1(2)}$ only 1s, 2s and 2p target two-body atomic wave-functions are included. This method represents a modified version of the close coupling approximation with six expansion functions. The set of truncated integral-differential Eqs. (23) is solved by a discretization

procedure, i.e. on the right side of the equations the integrals over ρ_1 and ρ_2 are replaced by sums using the trapezoidal rule [37] and the second order partial derivatives on the left side are discretized using a three-point rule [37]. By this means we obtain a set of linear equations for the unknown coefficients $f_\alpha^{(i)}(k)$ $(k = 1, N_p)$:

$$\left[k_n^{(1)2} + D_{ij}^2 - \frac{\lambda(\lambda+1)}{\rho_{1i}^2} \right] f_\alpha^{(1)}(i) \; - \; \frac{M_1}{\gamma^3} \sum_{\alpha'=1}^{N_s} \sum_{j=1}^{N_p} w_j S_{\alpha\alpha'}^{(12)}(\rho_{1i}, \rho_{2j}) f_{\alpha'}^{(2)}(j) = 0, \tag{40}$$

$$-\frac{M_2}{\gamma^3} \sum_{\alpha=1}^{N_s} \sum_{j=1}^{N_p} w_j S_{\alpha'\alpha}^{(21)}(\rho_{2i}, \rho_{1j}) f_\alpha^{(1)}(j) \; + \; \left[k_{n'}^{(2)2} + D_{ij}^2 - \frac{\lambda'(\lambda'+1)}{\rho_{2i}^2} \right] f_{\alpha'}^{(2)}(i) = B_{\alpha'}^{21}(i). \tag{41}$$

Here, coefficients w_j are weights of the integration points ρ_{1i} and ρ_{2i} $(i = 1, N_p)$, N_s is the number of quantum states which are taken into account in the expansion (14). Next, D_{ij}^2 is the three-point numerical approximation for the second order differential operator: $D_{ij}^2 f_\alpha(i) = (f_\alpha(i-1)\delta_{i-1,j} - 2f_\alpha(i)\delta_{i,j} + f_\alpha(i+1)\delta_{i+1,j})/\Delta$, where Δ is a step of the grid $\Delta = \rho_{i+1} - \rho_i$. The vector $B_{\alpha'}^{21}(i)$ is: $B_{\alpha'}^{(21)}(i) = M_2/\gamma^3 \sum_{j=1}^{N_p} w_j S_{\alpha' 1 s0}^{(21)}(i, j) \sin(k_1 \rho_j)$, and in symbolic-operator notations the set of linear Eqs. (40)-(41) has the following form:

$$\sum_{\alpha'=1}^{2\times N_s} \sum_{j=1}^{N_p} \mathbf{A}_{\alpha\alpha'}(i, j) \vec{f}_{\alpha'}(j) = \vec{b}_\alpha(i). \tag{42}$$

The discretized equations are subsequently solved by the Gauss elimination method [38]. As can be seen from Eqs. (40)-(41) the matrix **A** should have a so-called block-structure: there are four main blocks in the matrix: two of them related to the differential operators and other two to the integral operators. Each of these blocks should have sub-blocks depending on the quantum numbers $\alpha = nl\lambda$ and $\alpha' = n'l'\lambda'$. The second order differential operators produce three-diagonal sub-matrixes [31].

However, there is no need to keep the whole matrix **A** in computer's operating (fast) memory. The following optimization procedure shows that it would be possible to reduce the memory usage by at least four times. Indeed, the numerical equations (40)-(41) can be written in the following way: $D_1 f^1 - M_1 \gamma^{-3} S^{12} f^2 = 0$, and $-M_2 \gamma^{-3} S^{21} f^1 + D_2 f^2 = b$. Here, D_1, D_2, S^{12} and S^{21} are sub-matrixes of **A**. Now one can determine that: $f^1 = (D_1)^{-1} M_1 / \gamma^3 S^{12} f^2$, where $(D_1)^{-1}$ is reverse matrix of D_1. Thereby one can obtain a reduced set of linear equations which are used to perform the calculations: $\left[D_2 - M_1 M_2 \gamma^{-6} S^{21} (D_1)^{-1} S^{12} \right] f^2 = b$ [31].

To solve the coupled integral-differential equations (23) one needs to first compute the angular integrals Eqs. (22). They are independent of energy E. Therefore, one needs to compute them only once and then store them on a computer's hard drive (or solid state drive) to support future computation of other observables, i.e. the charge-transfer cross-sections at different collision energies.

The sub-integral expressions in (22) have a very strong and complicated dependence on the Jacobi coordinates ρ_i and $\rho_{i'}$. To calculate $S_{\alpha\alpha'}^{(ii')}(\rho_i, \rho_{i'})$ at different values of ρ_i and $\rho_{i'}$ an adaptable algorithm has been applied together with the following mathematical substitution: $\cos\omega = (x^2 - \beta_i^2 \rho_i^2 - \rho_{i'}^2)/(2\beta_i \rho_i \rho_{i'})$. The angle dependent part of the equation can be written as the following one-dimensional integral:

$$S_{\alpha\alpha'}^{(ii')}(\rho_i, \rho_{i'}) = \frac{4\pi}{\beta_i} \frac{[(2\lambda+1)(2\lambda'+1)]^{\frac{1}{2}}}{2L+1} \int_{|\beta_i\rho_i - \rho_{i'}|}^{\beta_i\rho_i + \rho_{i'}} dx R_{nl}^{(i)}(x) \left[-1 + \frac{x}{r_{ii'}(x)} \right] R_{n'l'}^{(i')}(r_{i3}(x)) \times \sum_{mm'} D_{mm'}^L(0, \omega(x), 0) C_{\lambda 0 lm}^{Lm} C_{\lambda' 0 l'm'}^{Lm'} Y_{lm}(\nu_i(x), \pi) Y_{l'm'}^*(\nu_{i'}(x), \pi). \tag{43}$$

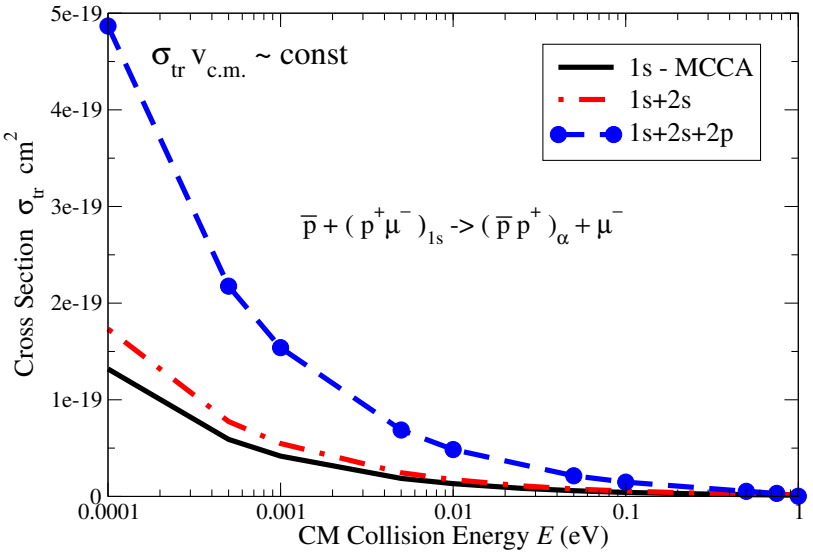

Figure 3. This figure shows our numerical result for the low-energy proton transfer reaction integral cross section σ_{tr} in the three-charge-particle collision $\bar{p} + H_\mu \rightarrow (\bar{p}p)_\alpha + \mu^-$, where H_μ is a muonic hydrogen atom: a bound state of a proton and a negative muon. In this work only the reaction final channel with α=1s in considered in the framework of the 1s, 1s+2s and 1s+2s+2p modified close-coupling approximation (MCCA) approach.

An adaptive algorithm which is incorporated in a FORTRAN subroutine from [39] is used in this work in order to carry out the angle integration in (43). This recursive computer program, QUADREC, is a better, modified version of the well known program QUANC8 [38]. QUADREC provides a much higher quality, stable and more precise integration than does QUANC8 [39]. The expression (43) differs from zero only in a narrow strip, i.e. when $\rho_i \approx \rho_{i'}$. This is because in the considered three-body system the coefficient β_i is approximately equal to one. Therefore, in order to obtain numerically reliable converged results it is necessary to adequately distribute a very large number of discretization points (up to 6000) between 0 and ~80 muonic units.

3 Results

In this section we report our computational results. The *Pn* formation three-body reaction is computed. A Faddeev-like equation formalism (6)-(7) has been applied. The few-body approach is presented in previous sections. In order to solve the coupled equations (6)-(7) two different independent sets of target expansion functions have been used (14). This method allows us to avoid the over-completeness problem and the two targets are treated equivalently. The main goal of this work is to carry out a reliable quantum-mechanical computation of the cross sections and corresponding rates of the title *Pn* formation reaction at low and very low collision energies. It would also be interesting to include and estimate a contribution of the strong $\bar{p}-p$ interaction. The coupled integral-differential Eqs. (23) have been solved numerically for the case of the total angular momentum $L = 0$ in the framework of the two-level 2×(1s), four-level 2×(1s+2s), and six-level 2×(1s+2s+2p) close coupling approximations in Eq. (14). The sign "2×" indicates that two different sets of expansion functions are applied. The following boundary conditions (35), (36), and (37) have been used. To compute the charge transfer cross

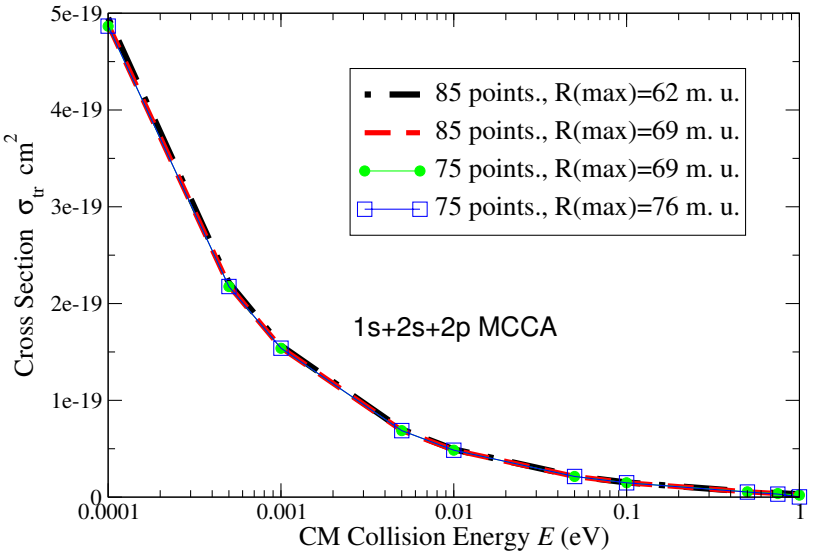

Figure 4. Numerical convergence results for the low-energy proton transfer reaction integral cross section σ_{tr} in $\bar{\mathrm{p}} + \mathrm{H}_\mu \rightarrow (\bar{\mathrm{p}}\mathrm{p})_\alpha + \mu^-$, where H_μ is a muonic hydrogen atom and α =1s . In these calculations only $1s + 2s + 2p$ modified close-coupling approximation (MCCA) approach is used.

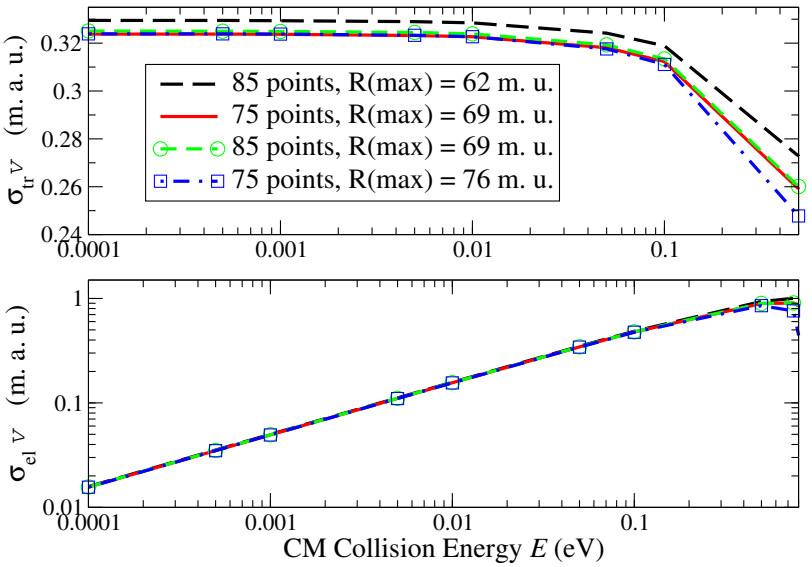

Figure 5. Numerical convergence results for the low-energy proton transfer reaction integral cross section σ_{tr} and elastic scattering cross section σ_{el} multiplied by the collision velocity in $\bar{\mathrm{p}} + \mathrm{H}_\mu \rightarrow (\bar{\mathrm{p}}\mathrm{p})_\alpha + \mu^-$, where H_μ is a muonic hydrogen atom and α =1s . In these calculations only $1s+2s+2p$ modified close-coupling approximation (MCCA) approach is used.

Table 1. The total *Pn* formation cross section σ_{tr} in the three-body reaction (3), when $\alpha = 1$, and a product of this cross section and the corresponding center-of-mass velocities $v_{c.m.}$ between $\bar{p}$ and H_μ. The results are prsented together with the corresponding unitarity ratio between the K_{12} and K_{21} coefficients of the scattering K-matrix.

	$2\times(1s)$ - MCCA Approach		$2\times(1s + 2s)$ - MCC Approach		
E, eV	σ_{tr}, cm^2	$\sigma_{tr}\times v_{c.m.}$, m.a.u	σ_{tr}, cm^2	$\sigma_{tr}\times v_{c.m.}$, m.a.u	$\chi(E)$, Eq. (39)
0.0001	0.1319E-18	0.8776E-01	0.1733E-18	0.1153	0.9976
0.0005	0.5897E-19	0.8776E-01	0.7749E-19	0.1153	0.9976
0.0010	0.4170E-19	0.8776E-01	0.5479E-19	0.1153	0.9976
0.0050	0.1865E-19	0.8776E-01	0.2450E-19	0.1153	0.9976
0.0100	0.1319E-19	0.8775E-01	0.1733E-19	0.1153	0.9976
0.0500	0.5895E-20	0.8773E-01	0.7748E-20	0.1153	0.9977
0.1000	0.4168E-20	0.8771E-01	0.5478E-20	0.1153	0.9977
0.5000	0.1860E-20	0.8753E-01	0.2450E-20	0.1153	0.9982

sections the expression (38) has been applied. The constructed equations satisfy the Schrődinger equation exactly. For the energies below the three-body break-up threshold they exhibit the same advantages as the Faddeev equations [24], because they are formulated for the wave function components with correct physical asymptotes. To solve the equations, a close-coupling method is applied, which leads to an expansion of the system's wave function components into eigenfunctions of the subsystem (target) Hamiltonians providing with a set of one-dimensional integral-differential equations after the partial-wave projection. A further advantage of the Faddeev-type method is the fact that the Faddeev-components are smoother functions of the coordinates than the total wave function.

Below we report our new computational results. We compare some of our findings with the corresponding data from older work [40]. The *Pn* formation cross section in the reaction (3) are shown in Fig. 3. Here we used only $1s$, $1s + 2s$ and $1s + 2s + 2p$ states within the modified close-coupling approximation (MCCA) approach. One can see that the contribution of the $2s$- and $2p$-states from each target is becoming even more significant while the collision energy becomes smaller. It would be useful to make a comment about the behaviour of $\sigma_{tr}(\varepsilon_{coll})$ at very low collision energies: $\varepsilon_{coll} \sim 0$. From our calculation we found that the p^+ transfer cross sections $\sigma_{tr} \to \infty$ as $\varepsilon_{coll} \to 0$. However, the p^+ transfer rates, λ_{tr}, are proportional to the product $\sigma_{tr} \times v_{c.m.}$ and this trends to a finite value as $v_{c.m.} \to 0$. Here $v_{c.m.} = \sqrt{2\varepsilon_{coll}/M_k}$ is a relative center-of-mass velocity between the particles in the input channel of the three-body reactions, and M_k is the reduced mass. To compute the proton transfer rate the following formula is used:

$$\lambda_{tr} = \sigma_{tr}(\varepsilon_{coll} \to 0)v_{c.m.} \tag{44}$$

Therefore, additionally, for the process (1) we compute the numerical value of the following important quantity: $\Lambda(Pn) = \lambda_{tr} = \sigma_{tr}(\varepsilon_{coll} \to 0)v_{c.m.} \approx$ const, which is proportional to the actual *Pn* formation rate at low collision energies. Table 1 includes our data for this important parameter together with the *Pn* formation total cross section. All these results are obtained in the framework of the $2\times(1s)$ and $2\times(1s + 2s)$ approximations. The sign "$2\times$" means, as we mentioned, that two sets of the expansion

functions from each target are applied. Therefore, for example, in the case of the $1s$ MCCA approach two expansion functions are used in our calculations. However, in the case of the $1s + 2s$ MCCA approach four expansion functions are applied. Additionally, as we mentioned above, the unitarity relationship, i.e. Eq. (39), is checked for all considered collision energies E. It is seen, that $\chi(E)$ posses a fairly constant value close to one. Figs. 4 and 5 show our convergence results. In these cases we used different number of integration points, namely 75 and 85 per one muonic radius length and different values of the up level of integration, namely 62, 69 and 76 m. a. u. Thus, the maximum amount of the integration number used in this work is $N_{max} = 76 \times 85 = 6460$. It is seen that the results are in a good agreement with each other for the transfer and elastic cross sections.

In the framework of the $2\times(1s + 2s + 2p)$ MCCA approach, i.e. when six coupled Faddeev-Hahn-type integral-differential equations are solved, our result for the Pn formation rate has the following value: $\Lambda_{1s2s2p}(Pn) = \sigma_{tr}\times v_{c.m.} \approx 0.32$ m.a.u. The corresponding rate from the work [40] is: $\Lambda'(Pn) \approx 0.2$ m.a.u. Both results are in a fairly good agreement with each other and were multiplied by *5* as in [40]. In conclusion, because of the complexity of the few-body system and the method, in this work only the total orbital momentum $L = 0$ has been taken into account. It was adequate in the case of the slow and ultraslow collisions discussed above. However, inclusion of the strong proton-antiproton interaction in this work by just shifting the ground state energy level of the Pn atom [13] increased our results by $\sim 50\%$. In a future work it would be useful to take into account higher atomic target states like 3s+3p+3d+4s+... as well as the continuum spectrum. This calculation would be an interesting investigation. However, at very low energy collisions, which are considered in this paper, all these channels are closed and located far away from the actual collision energies. At the same time the main contribution from s- and p-states (polarization) is taken into account. A direct inclusion of the strong $\bar{p}-p$ interaction [14, 15] would be a very interesting future investigation in the framework of the three-body reaction (3).

References

[1] M. Hori and J. Waltz, Prog. Part. Nucl. Phys. **72**, 206 (2013).
[2] W. A. Bertsche, E. Butler, M. Charlton, and N. Madsen, J. Phys. B: At. Mol. Opt. Phys. **48**, 232001 (2015).
[3] G. Gabrielse et al., (ATRAP Collaboration), Phys. Rev. Lett. **106** 073002 (2011).
[4] G. B. Andresen et al., (ALPHA Collaboration), Phys. Rev. Lett. **105** 013003 (2010).
[5] Y. Yamazaki and S. Ulmer, Ann. Phys. (Berlin), **525**, 493 (2013).
[6] R. S. Hayano, M. Hori, D. Horvath, and E. Widmann, Rep. Prog. Phys. **70**, 1995 (2007).
[7] M. Hori et al., Nature **475**, 484 (2011).
[8] N. Zurlo et al., (ATHENA Collaboration), Phys. Rev. Lett. **97**, 153401 (2006).
[9] L. Venturelli et al., Nucl. Instrum. Methods Phys. Res., Sect. B **261**, 40 (2007).
[10] E. L. Rizzini et al., Europ. Phys. J. Plus, **127**, 1 (2012).
[11] I. S. Shapiro, Phys. Rep. **35**, 129 (1978).
[12] J. Hrtánková and J. Mareš, Nucl. Phys. A **945**, 197 (2015).
[13] J. -M. Richard and M. E. Sainio, Phys. Lett. B **110**, 349 (1982).
[14] E. Klempt, F. Bradamante, A. Martin, J.-M. Richard, Phys. Rep. **368**, 119 (2002).
[15] E. Klempt, C. Batty, J.-M. Richard, Phys. Rep. **413**, 197 (2005).
[16] L. N. Bogdanova, O. D. Dalkarov, and I. S. Shapiro, Ann. Phys. **84**, 261 (1974).
[17] T. Barnes, AIP Conf. Proc. **796**, 53 (2005).
[18] X. M. Tong, K. Hino, N. Toshima, Phys. Rev. Lett. **97**, 243202 (2006).

[19] K. Sakimoto, Phys. Rev. A **88** 012507 (2013).
[20] B. D. Esry and H. R. Sadeghpour, Phys. Rev. A **67**, 012704 (2003).
[21] M. Born and R. Oppenheimer, Ann. Phys., Liepzig, **84**, 457 (1927).
[22] T. Ueda, Prog. Theor. Phys. **62**, 1670 (1979.)
[23] L. D. Faddeev, Zh. Eksp. Teor. Fiz. **39** 1459 (1960) [Sov. Phys. JETP **12** 1014 (1961)].
[24] L. D. Faddeev and S. P. Merkuriev, *Quantum Scattering Theory for Several Particle Systems*, (Kluwers Academic Publishers, Dordrecht, 1993); L. D. Faddeev, *Mathematical Aspects of the Three-Body Problem in the Quantum Scattering Theory*, (Israel, Program for Scientific Translation, Jerusalem, 1965).
[25] Y. Hahn and K. Watson, Phys. Rev. A **5** 1718 (1972).
[26] Y. Hahn, Nucl. Phys. A **389**, 1 (1982).
[27] R. A. Sultanov and S. K. Adhikari, Phys. Rev. A **61**, 227111 (2000).
[28] R. A. Sultanov and D. Guster, J. Phys. B: At. Mol. Opt. Phys. **46** 215204 (2013).
[29] R. A. Sultanov and D. Guster, Hyperfine Interact. **228**, 47 (2014).
[30] R. A. Sultanov, D. Guster, and S. K. Adhikari, Few-Body Syst. **56**, 793 (2015).
[31] R.A. Sultanov and D. Guster, J. Comp. Phys. **192**, 231 (2003).
[32] S. P. Merkuriev, Ann. Phys. **130**, 395 (1980).
[33] D. A. Varshalovich, A. N. Moskalev, and V. L. Khersonskii, *Quantum Theory of Angular Momentum*, (World Scientific, Singapore, 1988).
[34] A. Adamczak, C. Chiccoli, V. I. Korobov, V. S. Melezhik, P. Pasini, L. I. Ponomarev, and J. Wozniak, Phys. Lett. B **285**, 319 (1992).
[35] J.S. Cohen and M.C. Struensee, Physical Review A **43**, 3460 (1991).
[36] A. A. Kvitsinsky, J. Carbonell, C. Gignoux, Physical Review A **51**, 2997 (1995).
[37] M. Abramowitz and I. A. Stegun, *Handbook of Mathematical Functions: with Formulas, Graphs, and Mathematical Tables*, (Dover Publications, New York, 1965).
[38] G. E. Forsythe, M. A. Malcolm, and C. B. Moler, *Computer Methods in Mathematical Computations*, (Prentice-Hall, Inc., Englewood Cliffs, New Jersey 1977).
[39] A. N. Berlizov and A. A. Zhmudsky, arXiv:physics/9905035v2.
[40] A. Igarashi and N. Toshima, Eur. Phys. J. D **46**, 425 (2008).